KSCE Journal of Civil Engineering (2017) 21(7):2622-2633
DOI 10.1007/s12205-017-1010-2

Geotechnical Engineering
pISSN 1226-7988, eISSN 1976-3808
www.springer.com/12205

Nonlinear Analysis of Single Reinforced Concrete Piles Subjected to Lateral Loading

Ling-Yu Xu*, Fei Cai, Guo-Xin Wang***, Guo-Xing Chen****, and Yong-Yi Li*******

Received December 2, 2015/Accepted December 6, 2016/Published Online February 13, 2017

Abstract

This paper proposes a method for the nonlinear analysis of laterally loaded single reinforced concrete piles based on the beam-on-nonlinear-Winkler-foundation approach. A nonlinear fiber beam-column element is used to model the nonlinear behavior of a pile. The pile is divided into a series of segments, of which the cross section is assumed to be plane and normal to the longitudinal axis. The internal force of a segment is derived by integrating the nonlinear stress-strain relationships of all steel and concrete fibers within the cross section of the segment. The substructure technique is introduced to calculate the stiffness matrix of the segments. The nonlinear behavior of soils surrounding the pile is characterized by a modified strain wedge model. The results show that (1) the predicted results using the proposed method are consistent with the measurements for all three full-scale tested piles, and (2) updating the neutral axis of segments has a significant effect on the calculated lateral deflection; however, it has a slight effect on the calculated bending moment. Moreover, an empirical equation is derived from the numerical analyses for estimating the cracked flexural rigidity of bored piles subjected to lateral loading.

Keywords: *lateral load, reinforced concrete pile, neutral axis, nonlinear fiber beam-column element, cracked flexural rigidity*

1. Introduction

Piles are commonly used to transfer vertical (axial) forces, arising primarily from gravity (e.g., the weight of superstructures). However, the piles do not only carry the axial force. The piles are often subjected to either monotonic or cyclic lateral loading due to different hazards, such as the impact of ships on bridge piers during berthing, wave and wind actions on offshore structures, and seismic wave motion on different buildings (Poulos, 1977; Basu *et al*., 2008; Heidari *et al.*, 2013; Peng *et al.*, 2010).

The nonlinear behavior of a pile is normally considered for piles subjected to a large lateral load. Several procedures are employed for soil modeling in the numerical analysis of the nonlinear behavior of reinforced concrete piles, ranging from soil continuum discretization approaches to the beam-on-nonlinear-Winkler-foundation (BNWF) approach. The 3D finite element method, or finite difference method, which takes into account the three-dimensional soil–pile interaction and the nonlinear behavior of both soil and pile, has been frequently used to study the static and dynamic response of laterally loaded single piles and pile groups (Hsueh *et al.*, 2004; Giannakos *et al*., 2012; Tuladhar *et al*., 2008; Conte *et al*., 2013). Although the finite element method is the most versatile procedure for such a nonlinear problem, it remains generally unattractive in practice due to its complexity and presumed large computational efforts (El Naggar, 2005; Allotey and El Naggar, 2008; Memarpour *et al*., 2008).

The nonlinear behavior of a pile was originally considered in the *BNWF* approach by Reese (1984) to study piles subjected to static lateral loading. The Reese (1984) approach, which employs *p-y* curves to calculate the subgrade reaction modulus of soil, requires separate evaluation of the bending moment and curvature (M-Φ) relationship of the pile cross section and the adoption of a reduced flexural rigidity to replace the original pile flexural rigidity. Reese and Wang (1994) improved the Reese (1984) approach by computing the bending moment and the associated value of flexural rigidity at each increment of loading. The Reese and Wang (1994) approach was also adopted by Huang *et al.* (2001) to back calculate the lateral response of a reinforced concrete pile. Ashour *et al.* (2001) noted that the effect of the variation in the value of flexural rigidity of the pile on the subgrade reaction modulus is neglected in the Reese and Wang (1994) approach, and thus, a multi-layered beam-column element was used to model the nonlinear behavior of a pile.

In this study, a fiber beam-column element, in conjunction

*Lecturer, School of Transportation Science and Engineering, Nanjing Tech University, Nanjing 210009, China (Corresponding Author, E-mail: xulingyu2008@126.com)
**Assistant Professor, Dept. of Environmental Engineering Science, Gunma University, Kiryu 3768515, Japan (E-mail: feicai@gunma-u.ac.jp)
***Professor, School of Hydraulic Engineering, Dalian University of Technology, Dalian 116024, China (E-mail: gxwang@dlut.edu.cn
****Professor, School of Transportation Science and Engineering, Nanjing Tech University, Nanjing 210009, China (E-mail: gxc6307@163.com)
*****Associate Professor, School of Transportation Science and Engineering, Nanjing Tech University, Nanjing 210009, China (E-mail: liyongyi@njtech.edu.cn)

with the modified strain wedge model proposed by Xu *et al.* (2016), is employed to study the nonlinear behavior of reinforced concrete piles subjected to lateral monotonic loading. The cross section of segments, into which the pile is divided, is assumed to be plane and normal to the longitudinal axis. The cross section of segments is then discretized into longitudinal steel and concrete fibers. The internal force of a segment is derived by integrating the nonlinear stress-strain relationships of all steel and concrete fibers within the cross section of the segment. The substructure technique is introduced to calculate the stiffness matrix of the segments. The proposed method is verified by three case histories. Moreover, the proposed method is compared with a simplified design method using constant stiffness with a value equal to half of the initial flexural rigidity for the whole pile cross section. The effect of updating the neutral axis of segments on the lateral response of piles is discussed. Finally, an empirical equation is proposed to estimate the cracked flexural rigidity of bored piles subjected to lateral loading.

2. The Proposed Method

The governing differential equation for laterally loaded piles is given as follows:

$$EI\left(\frac{d^4y}{dx^4}\right)+E_s(x)y=0 \tag{1}$$

where EI is the flexural stiffness of the pile, y is the lateral deflection of the pile, and $E_s(x)$ is the subgrade reaction modulus at a depth of x, obtained using the Modified Strain Wedge (MSW) model proposed by Xu *et al.* (2016), which will be briefly presented in Section 2.1.

In this study, a nonlinear fiber beam-column element based on the Euler-Bernoulli beam theory is used for the finite element analysis of the nonlinear behavior of a pile, as will be presented in Section 2.2. Sign conventions for beam element positive nodal displacements, rotations, forces, and moments in the finite element method and for positive shear forces and bending moments in the beam theory are shown in Fig. 1. The substructure technique is introduced to calculate the stiffness matrix of segments. The modified Newton-Raphson method with an initial problem tangent is used for solutions in the FEM analysis. For details of the modified Newton-Raphson method, refer to Zienkiewicz and Taylor (2005). The proposed procedure has been incorporated in the SWPILE program (Xu *et al.*, 2013) for the analysis of laterally loaded single reinforced concrete piles.

2.1 Description of the MSW Model

The function of the MSW model is to calculate the soil resistance p based on the principle of force equilibrium. Then, the subgrade reaction modulus, E_s, at the face of the MSW can be calculated by using the following equation (Prakash and Kumar, 1996):

$$E_s=\frac{p}{y} \tag{2}$$

where y is the pile deflection, obtained from the *BNEF* analysis.

The MSW in front of the pile is characterized by a base angle β_m for single layers or base angles for multiple layers, a fan angle $\eta\varphi_m$, and a wedge height, as shown in Fig. 2. φ_m is the mobilized effective friction angle and η is the coefficient. $\eta = 1$ and $\eta = 0.2$ are adopted for sands (Xu *et al.*, 2013) and clays (Kim *et al.*, 2011; Xu *et al.*, 2016), respectively. The soil in the MSW is divided into sublayers. The hyperbolic stress - strain relationship is used to describe the relation between horizontal stress change and the horizontal strain in the MSW. An array of discrete springs representing the soil is used to account for the soil-pile interaction. Nonlinear and linear springs are used in the MSW and below the MSW for flexible piles, respectively (Xu *et al.*, 2016).

2.2 Modeling the Nonlinear Behavior of a Reinforced Concrete Pile

A nonlinear fiber beam-column element is used to model the nonlinear behavior of a pile that is divided into a series of segments. It is assumed that the cross sections of segments

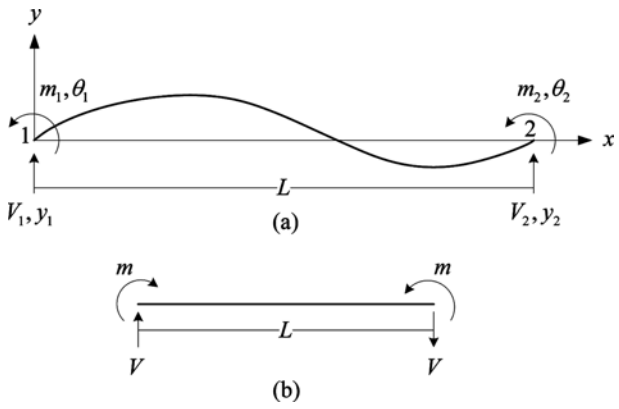

Fig. 1. Sign Conventions for (a) Beam Element with Positive Nodal Displacements (y), Rotations (θ), Forces (V), and Moments (m) in FEM and for (b) Positive Shear Forces (V) and Bending Moments (m) in Beam Theory

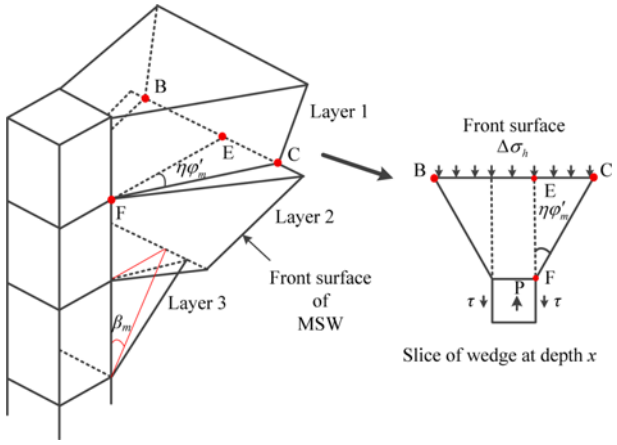

Fig. 2. Modified Strain Wedge (MSW), Consisting of Multiple Layers

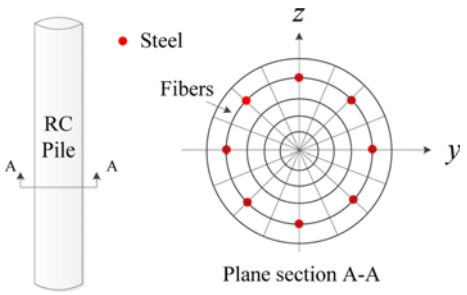

Fig. 3. Fiber Element Discretization of the Plane Section of a Reinforced Concrete (RC) Pile

remain plane and normal to the longitudinal axis. The effect of bond-slip is, thus, presently neglected. The cross section of segments is then discretized into longitudinal steel and concrete fibers, as shown in Fig. 3. The internal force of a segment is derived by integrating the nonlinear stress-strain relationships of all steel and concrete fibers within the cross section of the segment. The stress-strain relationship of the steel and concrete fibers will be presented below. Note that the beam is assumed to be in a state of plane stress; thus, the only nonzero stress is available in the longitudinal direction of fibers (Fish and Belytschko, 2007). In addition, the neutral axis on the cross section of segments is updated in every iteration step to obtain more accurate flexural rigidity of piles when the pile reaches the nonlinear state.

2.2.1 Stress-strain Relationship of Steel Fibers

A bilinear stress-strain relationship is considered in this study for steel fibers, as shown in Fig. 4, and is expressed in the following equation:

$$f_s = \begin{cases} E_s \varepsilon_s, & |f_s| < f_y \\ f_y, & |f_s| \geq f_y \end{cases} \tag{3}$$

where f_s is the steel stress, E_s is the elastic modulus of steel fibers, and f_y is the yield stress of steel. In this study, the sign convention of the stresses in fibers is as follows: tensile stress is positive and compressive stress is negative.

2.2.2 Stress-strain Relation of Concrete Fibers

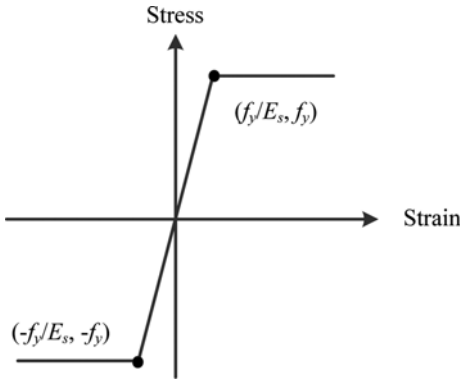

Fig. 4. Bilinear Stress-strain Relationship Considered for Steel Fibers

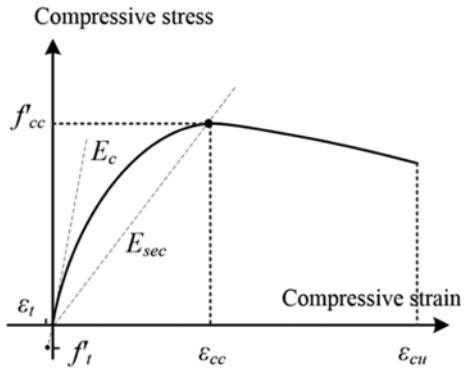

Fig. 5. Stress-strain Relationship Considered in Present Study for Compressive Concrete Fibers

A stress-strain relationship developed for compressive confined concrete under a slow strain rate and monotonic loading by Mander *et al.* (1988) is adopted in this study for compressive concrete fibers, as shown in Fig. 5.

The compressive stress in concrete f_c is given by:

$$f_c = \frac{f'_{cc} x r}{r - 1 + x^r} \tag{4}$$

where f'_{cc} is the compressive strength of confined concrete, and x and r are expressed as follow:

$$x = \frac{\varepsilon_c}{\varepsilon_{cc}} \tag{5}$$

$$r = \frac{E_c}{E_c - E_{sec}} \tag{6}$$

where ε_c is the longitudinal compressive concrete strain, ε_{cc} is the longitudinal compressive concrete strain at the compressive strength of confined concrete f'_{cc}, E_c is the elastic modulus of concrete, and E_{sec} is the secant modulus of confined concrete fibers at the compressive strength of confined concrete f'_{cc}.

The longitudinal compressive concrete strain at the compressive strength of confined concrete ε_{cc} is given as:

$$\varepsilon_{cc} = \varepsilon_{co}\left[1 + 5\left(\frac{f'_{cc}}{f'_{co}} - 1\right)\right] \tag{7}$$

where f'_{co} is the compressive strength of unconfined concrete, and ε_{co} is the longitudinal compressive concrete strain at the compressive strength of unconfined concrete. Generally, ε_{co} = 0.002 can be assumed (Mander *et al.*, 1988).

The elastic modulus of concrete E_c can be calculated by using an empirical expression (Mander *et al.*, 1988):

$$E_c = 5000\sqrt{f'_{co}}\ (\text{MPa}) \tag{8}$$

where the term f'_{co} is in MPa.

The secant modulus of concrete E_{sec} is expressed as:

$$E_{sec} = \frac{f'_{cc}}{\varepsilon_{cc}} \tag{9}$$

The longitudinal compressive concrete strain at the compressive strength of confined concrete f'_{cc} is given by:

$$f'_{cc} = f'_{co}\left(-1.254 + 2.254\sqrt{1+\frac{7.94 f'_l}{f'_{co}}} - 2\frac{f'_l}{f'_{co}}\right) \quad (10)$$

$$f'_l = \frac{1}{2} k_e \rho_s f_y \quad (11)$$

where f_l' is the effective lateral confining stress on concrete, k_e is the confinement effectiveness coefficient, and ρ_s is the ratio of volume of transverse confining steel to volume of confined concrete core. In this study, ρ_s is assumed to be 0.005. k_e is assumed to be 0.5 due to the lack of plausible data of piles in the analyzed case histories.

A conservative and simple equation for estimating the confined concrete ultimate strain is given by Paulay and Priestley (1992):

$$\varepsilon_{cu} = 0.004 + \frac{1.4\rho_s f_y \varepsilon_{su}}{f'_{cc}} \quad (12)$$

where ε_{su} is the steel strain at maximum tensile stress. Typical values for ε_{su} range from 0.012 to 0.05 (Chen and Duan, 2003).

According to Mander *et al.* (1988), a linear stress-strain relation is assumed in tension up to the tensile strength of concrete f_t', and the longitudinal tensile stress in concrete is assumed to be equal to zero when the tensile stress is greater than the tensile strength of concrete f_t'. Thus, the longitudinal tensile stress in concrete f_t is given by

$$f_t = \begin{cases} E_c \varepsilon_t, & f_t \le f'_t \\ 0, & f_t > f'_t \end{cases} \quad (13)$$

where E_c is the elastic modulus of concrete, and ε_t is the longitudinal tensile concrete strain. The tensile strength of concrete without reinforcement is approximately 5-10% of its compressive strength (Heiniö, 1999).

2.2.3 Updating the Neutral Axis on the Cross Section of Segments

The neutral axis of the cross section of segments is at $y = 0$ before the fiber yields, as shown by the beam element in the local reference system in Fig. 6, where m is the resultant moment. The resultant moment is defined as the product of the force and moment arm and expressed as:

$$m = -\int_A y f_t dA \quad (14)$$

where f_t symbolizes the longitudinal stress of steel and concrete fibers, $f_t dA$ is the force on the area dA, and y is the moment arm. The right-hand rule convention has been used for the moment.

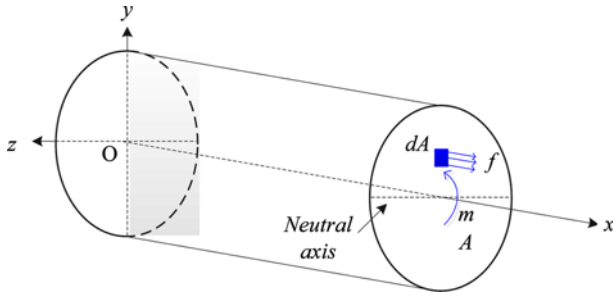

Fig. 6. Neutral Axis on the Cross Section of Each Segment in the Local Reference System

The negative sign appears in the expression because the moment is negative when the stress is positive for $y > 0$ (Fish and Belytschko, 2007).

In every iteration step, the binary search algorithm process is employed to determine the position of the neutral axis on the cross section of each segment when fibers in the associated cross section yield. Accordingly, the process is to maintain the following item (m_{ns}) smaller than a tolerant error (*Tot*) in FEM analysis.

$$m_{ns} = \int_A |y| f_t dA \le Tot \quad (15)$$

which is obtained by reforming Eq. (14). $Tot = 10^{-6}$ is used in this study.

Compared with *BNWF* approaches based on *p-y* curves or multi-layered beam-column element, the proposed method allows for more accurate and effective calculation of lateral response of RC piles by considering the nonlinear interaction between flexural rigidity of piles and subgrade reaction modulus, as presented in the following section. Note that the proposed method currently only applies to flexible piles in which the pile deflection below the MSW is small. Thus, the application of the proposed method to rigid piles needs further study of subgrade reaction modulus below the MSW.

3. Analysis of Case Histories

In this section, the validity of the proposed method is verified by comparing the results from the present approach with those from three full-scale pile tests and those from earlier research. The pile and soil properties are shown in Table 1 and Table 2, respectively.

3.1 Reuss *et al.* (1992) Case

Reuss *et al.* (1992) reported a full-scale reinforced concrete

Table 1. The properties of the Reinforced Concrete Pile Used for Three Case Histories in the SWPILE Program

Case histories	Diameter (m)	Concrete			Steel	
		E_c (MPa)	f'_{co} (MPa)	f'_t	E_s (GPa)	f_y (MPa)
Reuss *et al.* (1992)	0.406	32.2	-41.4	4.14	200	350
Liang (1997)	1.22	25.6	-41.2	4.12	200	460
Huang *et al.* (2001)	1.5	20.2	-27.5	2.7	200	471

Table 2. Soil Properties Used for Three Case Histories in the SWPILE Program

Case histories	No. of layers	Layer thickness (m)	Soil description	Total unit weight (kN/m^3)	S_u (kN/m^2)	ε_{50}	φ' (deg.)
Reuss *et al.* (1992)	1	1.8	Compacted gravelly clay	18.1	67	0.005	22
	2	11.3	Normally consolidated soft silty clay	18.9	29	0.02	22
	3	6.8	Normally consolidated soft to stiff clay	18.9	30	0.01	22
	4	2.1	Over consolidated stiff to hard clay	18.9	72	0.005	22
Liang (1997)	1	0.9	Brown sand, silt, clay	20	220	0.005	30
	2	0.9	Brown sand, silt, clay	21	241	0.004	30
	3	1.2	Gray weathered clay shale	22	311	0.005	30
	4	1.6	Gray weathered clay shale	22	690	0.003	30
	5	1.4	Argillaceous clay shale	22	1033	0.001	30
	6	4	Argillaceous clay shale	22	2067	0.001	30
	7	2	Shale, dark-gray, firm, fissile, broken and jointed	22	2067	0.001	30
Huang *et al.* (2001)	1	8	Fine sandy silt, silty fine sand	19	-	-	35
	2	4	Silty clay	19	60	0.007	28
	3	13	Silty fine sand	19	50	-	34
	4	9	Clayey silt	19	120	0.005	28

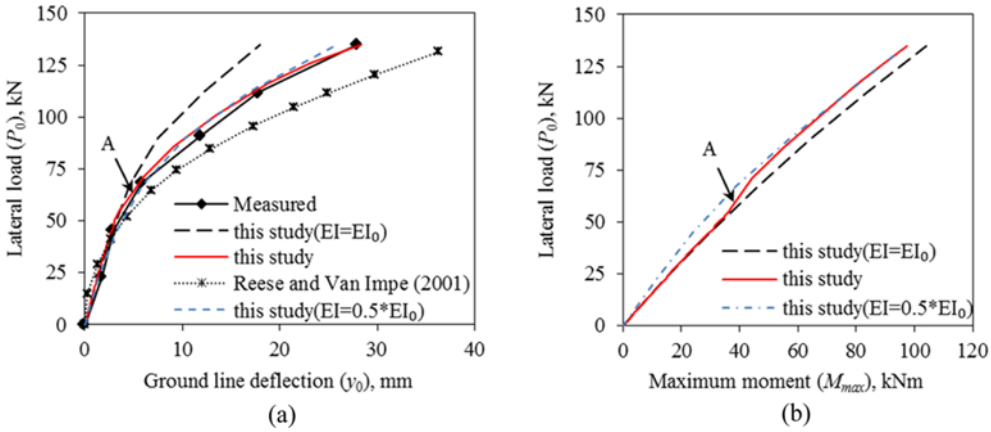

Fig. 7. The Predicted (a) Load-deflection Curves and (b) Load-maximum Moment Curves, Compared with the Measurements and the Results Predicted by Reese and Van Impe (2001) for the Case of Reuss *et al.* (1992)

pile tested at the Pyramid building site, Memphis. The longitudinal reinforcement and thickness of the concrete cover of the pile are taken as 3.0% and 25 mm, respectively (Ashour *et al.*, 2001). As a result, the initial flexural rigidity of the pile is calculated to be 51.9 MNm^2.

Figures 7(a) and 7(b) show the predicted load-deflection curves and load-maximum moment curves, respectively, compared with the measurements and the results predicted by Reese and Van Impe (2001). The deflections are underestimated for a lateral load above point A, as shown in Fig. 7(a), when using constant stiffness with a value equal to the initial flexural rigidity EI_0 for the whole pile cross section. This is because the concrete of the pile cracked at point A. However, when considering the nonlinear behavior of pile material, the predicted deflections correspond well with the measurements. Moreover, the proposed method can predict the deflections much better than those predicted by Reese and Van Impe (2001) using the *p-y* method. It is worth noting that when the concrete of the pile cracked, the

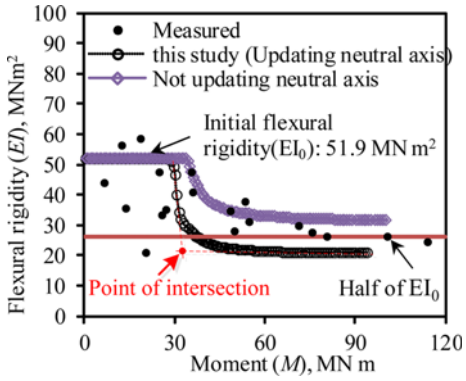

Fig. 8. Predicted and Measured Flexural Rigidities of the Pile for the Case of Reuss *et al.* (1992)

predicted moments considering the nonlinear behavior of the pile material became smaller than those considering the linear behavior of the pile material, as shown in Fig. 7(b). Moreover,

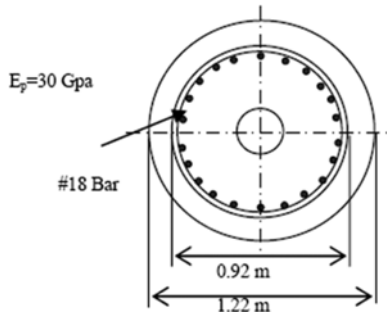

Fig. 9. Cross Section of a Full-scale Shaft Tested at the Ohio LOR-6 Test Site (Liang *et al.*, 2007)

the predicted flexural rigidities are in the range of the measurements, as shown by the predicted and measured *M-EI* relationships in Fig. 8. The results using constant stiffness with a value equal to half of the initial flexural rigidity EI_0 for the whole pile cross section are also depicted in Fig. 7 and will be presented in figures for the following case histories, as discussed in Section 4.

3.2 Liang (1997) Case

Liang *et al*. (2007) reported a full-scale shaft tested by Liang (1997) at the Ohio LOR-6 Test Site. The shaft was reinforced with a built-up steel pipe and 22 ϕ18 steel bars enclosed by the pipe, as shown in Fig. 9. The longitudinal reinforcement ratio is estimated to be approximately 2.5% by adding the area of the pipe equally to the area of each bar. As a result, the initial flexural rigidity of the pile is calculated to be 3.26 MNm^2, which was reported by Liang *et al.* (2007).

Figures 10(a) and 10(b) show the predicted load-deflection curves and load-maximum moment curves, respectively, compared with the measurements and the results predicted by Liang *et al.* (2007) using Liang *et al*. (2007) and Reese and Welch (1975) *p-y* curves. The predicted deflections correspond well with the measurements. Moreover, the predicted distributions of the deflection under three different lateral loads (i.e., 222 kN, 1100 kN, and 2580 kN) agree well with the measurements, as shown

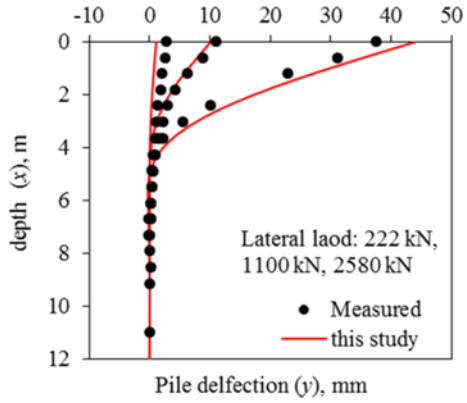

Fig. 11. Comparison of the Measured and Predicted Distributions of the Deflection under Three Different Lateral Loads for the Case of Liang (1997)

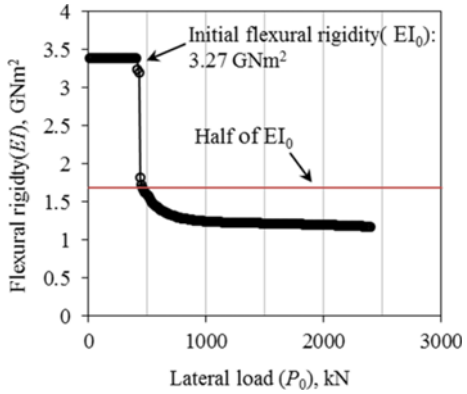

Fig. 12. Relationship between the Flexural Rigidity of the Pile Cross Section with Maximum Moment and the Lateral Load for the Case of Liang (1997)

in Fig. 11. However, the predicted maximum moments are much smaller than the measurements for a lateral load larger than approximately 1900 kN. The discrepancy between the predictions and the measurements may be due to the different methods used for the calculation of the bending moment in reinforced concrete

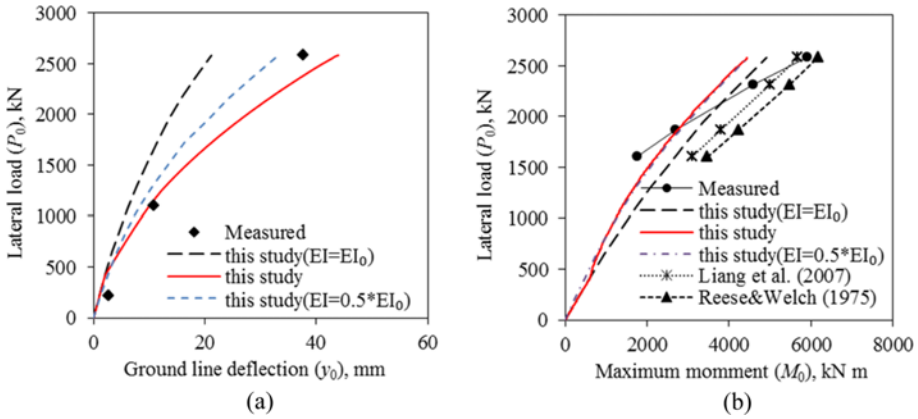

Fig. 10. The Predicted (a) Load-deflection Curves and (b) Load-maximum Moment Curves, Compared with the Measurements and Results Predicted by Liang *et al.* (2007) using Liang *et al.* (2007) and Reese and Welch (1975) *p-y* Curves for the Case of Liang (1997)

piles (Biocchi, 2011).

The cracked load (i.e., the load under which the concrete of the pile cracked) calculated in this study is approximately 432 kN, as shown in Fig. 12. The calculated cracked load is quite consistent with that observed from the measured load-deflection curves at the shaft top presented by Liang *et al*. (2007), i.e., approximately 500 kN. This indicates that the proposed method may give a more economic design for a reinforced concrete pile subjected to lateral loading because the maximum moments associated with the cracked load are largely overestimated by the Liang *et al*. (2007) and Reese and Welch (1975) *p-y* criteria, as shown in Fig. 10(b).

3.3 Huang *et al.* (2001) Case

Huang *et al.* (2001) performed full-scale load tests on two pile groups and some single piles to optimize the design of the pile foundations planned for the construction of a high-speed rail system in Taiwan. In this study, the results from a lateral loading test performed on a bored single reinforced concrete pile, denoted as B7, are considered. This pile was 1.5 m in diameter and 34.9 m in length. The reinforcement consisted of 52 ϕ32 steel bars arranged in two rings. The arrangement of the reinforcement assumed in this study is shown in Fig. 13. Making use of the *y*-axis of symmetry, only half of the plane section is used in the analysis. The ground-water table of the test site was located approximately 1 m below the ground surface (Huang *et al.*, 2001).

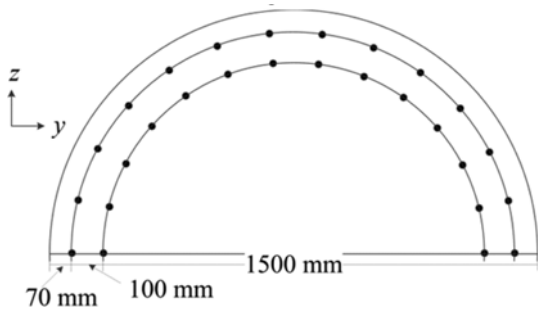

Fig. 13. Assumed Reinforcement for Pile B7 in this Study

Figures 14(a) and 14(b) show the measured and predicted load-deflection curves, respectively, compared with the measurements and results predicted by Conte *et al.* (2013). The predicted deflections correspond well with the measurements, as well as those calculated by Conte *et al.* (2013) using the finite element

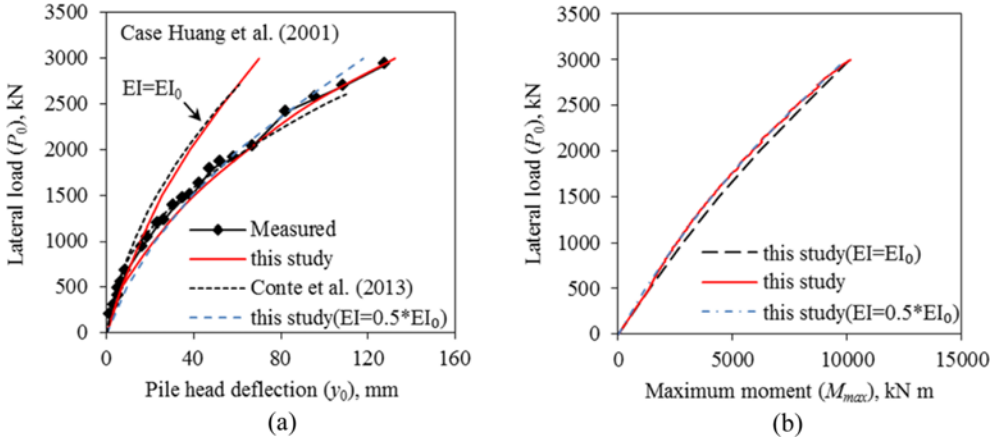

Fig. 14. The Predicted (a) load-deflection curves and (b) load-maximum moment curves, compared with the measurements and results predicted by Conte *et al.* (2013) for the case of Huang *et al.* (2001)

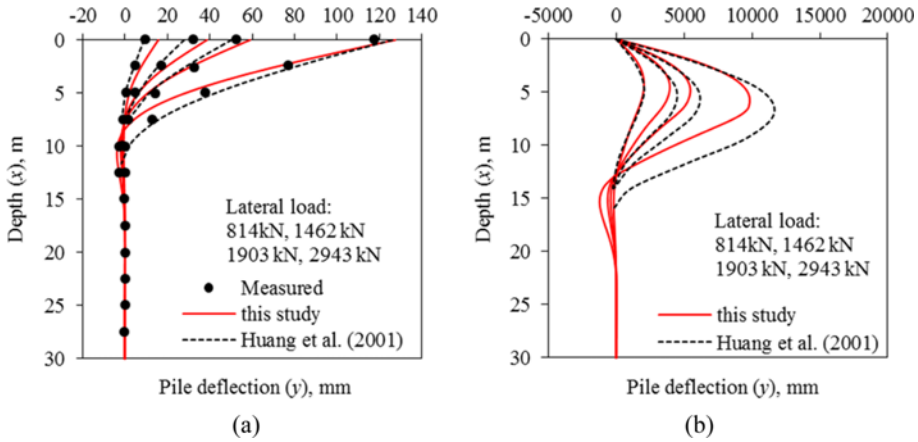

Fig. 15. The Predicted (a) Deflections and (b) Moments Along the Pile under four Lateral Loads, Compared with the Measurements and Those Predicted by Huang *et al.* (2001) using the *p-y* Method

code ABQUS. The results indicate that if constant stiffness with a value equal to the initial flexural rigidity EI_0 are used for the whole pile cross section, the deflections would be largely underestimated.

Figures 15(a) and 15(b) show the predicted deflections and moments along the pile, respectively, under four different lateral loads. The predicted deflections correspond well with the measurements and those predicted by Huang *et al.* (2001) using the *p-y* method, as shown in Fig. 15(a). Moreover, there is a good agreement between the moments predicted in this study and those predicted by Huang *et al.* (2001) for a lateral load of 814 kN. However, the agreement between the moments predicted using these two methods is generally satisfactory for the other three lateral loads. Nevertheless, the comparisons indicate that the proposed method can give reasonably good distributions of deflections and moments for laterally loaded reinforced concrete piles.

To evaluate the progressive cracking of concrete, some numerical results are presented in Figs. 16-18. According to the test results reported by Huang *et al.* (2001), there was a sharp change in curvature at 7-10 m below the ground surface under a lateral load of 1462 kN. The same effect was also found in the tested pile at depths between 4.5-5 m under a lateral load of 570 kN. This was because the concrete of the pile cracked at those depths, as discussed by Huang *et al.* (2001). Figs. 16(a) and 16(b) show the predicted flexural rigidity and moment along the pile, respectively, under lateral loads of 570 kN and 1462 kN. The results indicate that the moment reached its maximum at a depth of approximately 4.5 m under a lateral load 570 kN, as shown in Fig. 16(b). As a result, the concrete of the pile first cracked at a depth of approximately 4.5 m, and consequently, the flexural rigidity reached its minimum, as shown in Fig. 16(a). Moreover, the cracking became enlarged in the concrete involving the upper portion of the pile up to a depth of approximately 9.7 m when the lateral load reached 1462 kN, which is also consistent with the measurement reported by Huang *et al.* (2001).

Figure 17 shows that the flexural rigidity of the pile cross section with maximum moment starts to decrease as the lateral load increases when the lateral load is larger than approximately 500 kN due to the cracking of concrete. Fig. 18 shows longitudinal concrete stress contours of the pile cross section with maximum moment under three different lateral loads. The pile behaves linearly under a lateral load of 450 kN; thus, the compressive and tensile longitudinal stresses are symmetrically distributed on the left and right sides of the *z*-axis on the pile cross section, i.e., the neutral axis is at $y = 0$, as shown in Fig. 18(a). After the cracking of concrete occurs, the neutral axis gradually moves apart from the *z*-axis to the compressive side, as shown by Figs. 18(b) and 18(c).

Figure 19 shows the calculated stress–strain relationship for steel fiber and concrete fiber, the positions of which are shown by points A, B, C, and D in Fig. 18(a), on the pile cross section with the maximum moment. The largest compressive stress calculated for the concrete is approximately 26.6 MPa, which is lower than its compressive strength (27.5 MPa). However, the tensile stress of the steel fiber reached the maximum value at failure, indicating that the steel yielded during the test.

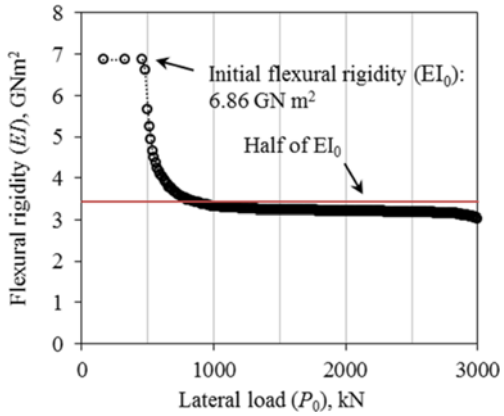

Fig. 17. Relationship between the Flexural Rigidity of the Pile Cross Section with Maximum Moment and the Lateral Load in the Case of Huang *et al.* (2001)

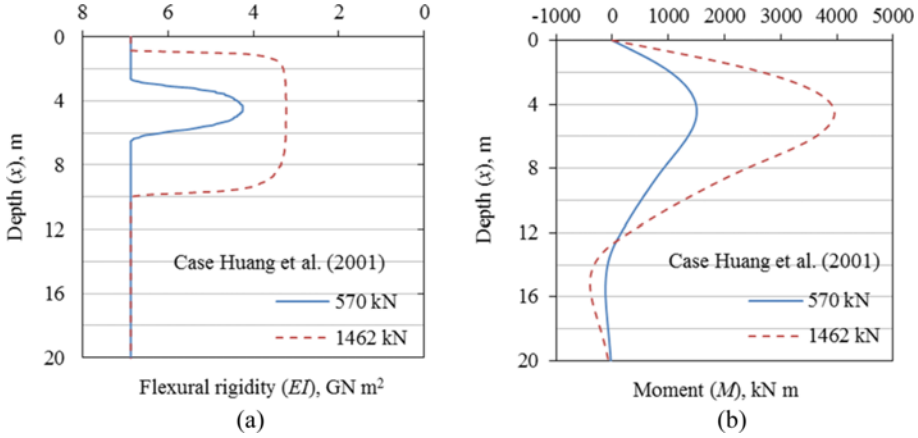

Fig. 16. The Predicted (a) Flexural Rigidity and (b) Moment Along the Pile Under Lateral Loads of 570 kN and 1462 kN

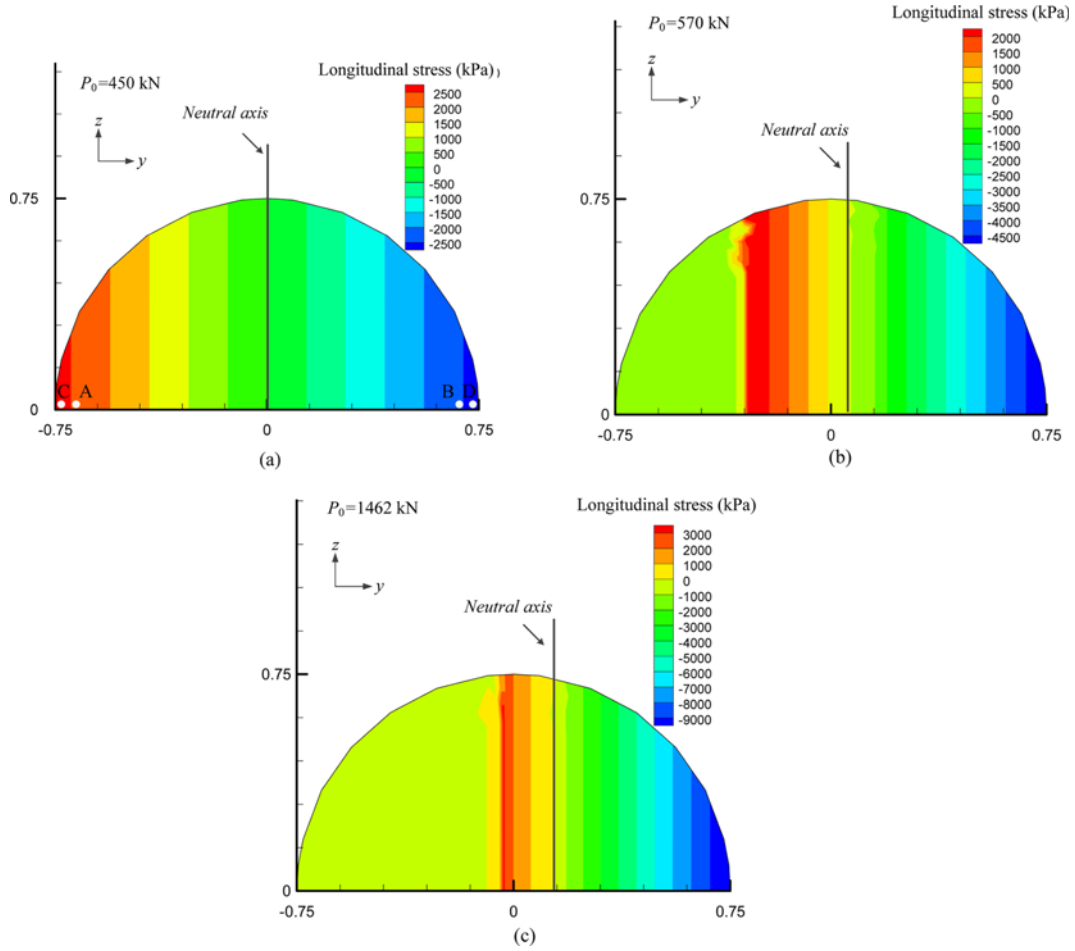

Fig. 18. Longitudinal Concrete Stress Contour of the Pile Plane Section with Maximum Moment under Lateral Loads of (a) 450 kN, (b) 570 kN, (c) 1462 kN

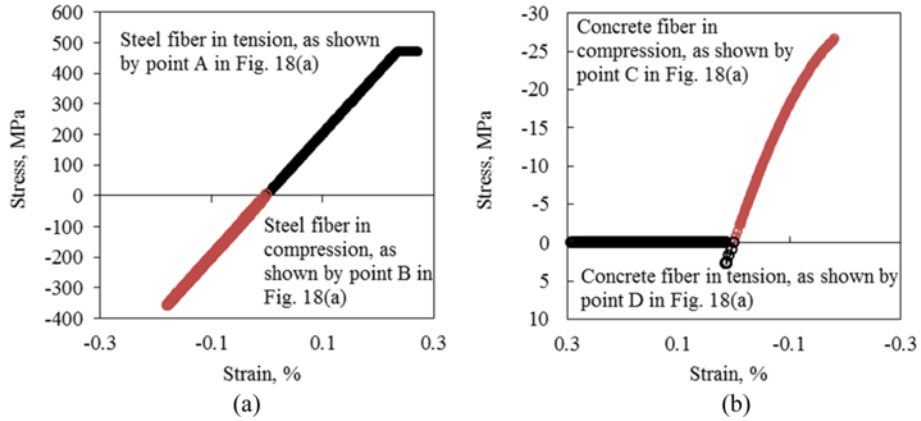

Fig. 19. Calculated Stress–strain Relationship for: (a) Steel Fiber (see Points A and B in Fig. 18(a)), (b) Concrete Fiber (see Points C and D in Fig. 18(a)) on the Pile Cross Section at the Maximum Moment

4. Discussions

4.1 Effect of Updating the Neutral Axis of Segments on the Lateral Response of Piles

Updating the neutral axis of segments can affect the calculated flexural rigidity of a pile and consequently the lateral response of the pile. Fig. 8 shows that the calculated results of the cracked flexural rigidities of the pile considering the update of the neutral axis are smaller than those not considering the update of the neutral axis. Fig. 20 shows the effect of updating the neutral axis of segments on the lateral response of the pile in the case of Reuss *et al.* (1992). In the case where the neutral axis is updated,

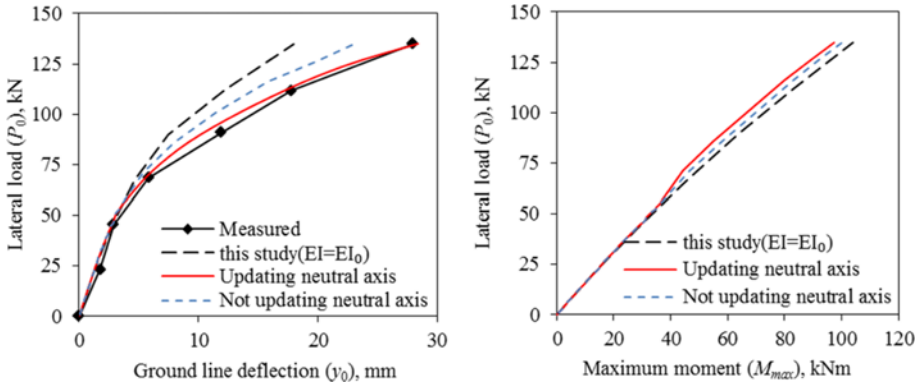

Fig. 20. Effect of Updating the Neutral Axis of Segments on the Lateral Response of the Pile in the Case of Reuss *et al.* (1992)

the ground line deflection is increased by approximately 23%, and the maximum bending moment is reduced by approximately 3% under a given maximum lateral load. Thus, updating the neutral axis of segments has a significant effect on the calculated lateral deflection; however, it has a slight effect on the calculated bending moment.

4.2 Comparison of the Proposed Method with a Simplified Design Method

In some routine designs, the value of flexural stiffness EI_0 of a cracked section is usually taken as half the value of an uncracked section for a simplified design (Nip and Ng, 2005). In this study, the above three case histories are also analyzed by using constant stiffness with a value equal to half of the initial flexural rigidity EI_0 for the whole pile cross section. This procedure is designated as a Simplified Design Method (SDM) analysis.

The predicted load - deflection and load - maximum moment curves using the SDM analysis are superimposed in Figs. 9, 10, and 14. The results show that the difference in the maximum moments calculated by these two methods is insignificant for these three case histories. However, the results indicate that the predicted deflections using the proposed method are first smaller and then larger than those using the SDM analysis when the lateral load exceeds a critical value. This is because the flexural rigidity of the pile calculated by the proposed method can decrease to the value less than half of the initial flexural stiffness when the lateral load exceeds the critical value, as shown in Figs. 8, 12, and 17. Thus, it is necessary to accurately estimate the cracked flexural rigidity of reinforced concrete piles for SDM analysis.

4.3 An Empirical Equation for Estimating the Cracked Flexural Rigidity of Bored Piles

To estimate the cracked flexural rigidity of bored piles, a series of numerical simulations is conducted for the case of Reuss *et al.* (1992) by changing the longitudinal reinforcement ratio and the compressive strength and elastic modulus of concrete used in the case of Reuss *et al.* (1992). The used longitudinal reinforcement ratios are 2.0%, 3.0%, 4.0%, 5.0%, and 6.5%, which are in the scope of the reinforcement ratio specified for bored piles in the Technical code for building pile foundation of China (Technical code for building pile foundation of China, JGJ 94 – 2008). The grades of concrete used in the simulation are C20, C30, C40, and C50. Thus, a total of 20 cases are analyzed.

The calculations show that the cracked flexural rigidity EI_c for the analyzed 20 cases increases as either the longitudinal reinforcement ratio ρ_l or the compressive strength of concrete f_{co}' increases. The cracked flexural rigidity EI_c is determined by the point of intersection of two broken lines that are obtained from the *EI*-*M* relationship using the linear square method, as shown in Fig. 8. However, the ratio of the cracked flexural rigidity EI_c to the initial flexural rigidity EI_0 generally decreases as the compressive strength of concrete f_{co}' increases. Fig. 21 shows the relation between EI_c/EI_0 and $\rho_l E_s/E_c$ for the 20 analyzed cases, from which an empirical equation is derived for bored piles, as expressed in the following equation:

$$EI_c = n_1 \left(\frac{\rho_l E_s}{E_c} \right)^{n_2} EI_0 \quad (2\% \le \rho_l \le 6.5\%) \tag{16}$$

where EI_c is the cracked flexural rigidity, ρ_l is the longitudinal reinforcement ratio, E_s is the elastic modulus of steel and usually taken as 200 GPa, E_c is the elastic modulus of concrete and

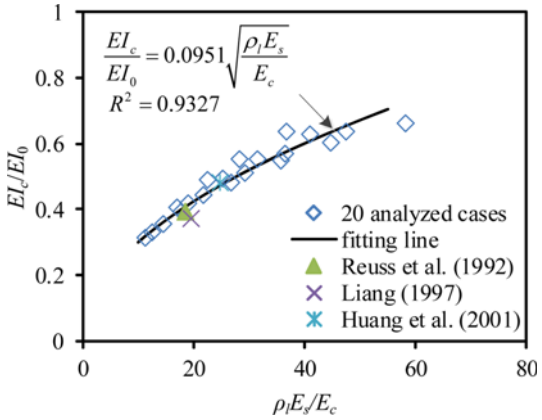

Fig. 21. The relationship between EI_c/EI_0 and $\rho_l E_s/E_c$ for the 20 Analyzed Cases and the Case of Reuss *et al.* (1992), Liang (1997), and Huang *et al.* (2001)

determined from Eq. (8) using the compressive strength of concrete f'_{co}, EI_0 is the initial flexural rigidity of piles, and n_1 and n_2 are fitting parameters taken as 0.0951 and 0.5, respectively.

The relationships between EI_c/EI_0 and $\rho_l E_s/E_c$ for the case of Reuss *et al.* (1992), Liang (1997), and Huang *et al.* (2001) are also given in Fig. 21. It is found that the cracked flexural rigidities for these three cases can be well estimated by the proposed empirical equation.

5. Conclusions

This paper proposes a method for the nonlinear analysis of laterally loaded single reinforced concrete piles based on the beam-on-nonlinear-Winkler-foundation approach. A nonlinear fiber beam-column element is used to model the nonlinear behavior of a pile. The pile is divided into a series of segments, of which the cross section is assumed to be plane and normal to the longitudinal axis. The internal force of a segment is derived by integrating the nonlinear stress-strain relationships of all steel and concrete fibers within the cross section of the segment. The substructure technique is introduced to calculate the stiffness matrix of the segments. The nonlinear behavior of soils surrounding the pile is characterized by a modified strain wedge model. The proposed method is verified using three case histories. Moreover, the proposed method is compared with a simplified design method with constant stiffness at a value equal to half of the initial flexural rigidity for the whole pile cross section. From the analysis of three full-scaled reinforced concrete piles, the following conclusions can be obtained:

1. The predicted results using the proposed method are consistent with the measurements for all three full-scale tested piles.
2. The concrete of piles in the three case histories cracked when the ground deflection of the piles is in the range of 2.0 mm ~ 10.0 mm. The pile deflection could be significantly underestimated in the case where the behavior of pile materials was assumed linear.
3. The predicted moments considering the nonlinear behavior of the pile material became smaller than those not considering the nonlinear behavior of the pile material when the concrete of the pile cracked.
4 The distribution of compressive and tensile stress was symmetrical on the cross section of the pile until the concrete of the pile cracked. Then, the calculated neutral axis of the pile cross section moved to the compressive side of the cross section.
5. Updating the neutral axis of segments has a significant effect on the calculated lateral deflection; however, it has a slight effect on the calculated bending moment.
6. The cracked flexural rigidity for bored piles can be well correlated with the longitudinal reinforcement ratio, the elastic modulus of concrete and steel, and the initial flexural rigidity using a power function.

Acknowledgements

This research was supported by the Natural Science Foundation of Jiangsu Province of China (Grant No. BK20150958), the National Natural Science Foundation of China (Grant Nos. 51508271, 51308291), and Postdoctoral Science Foundation of Jiangsu Province, China (Grant No. 1501067B) and China (Grant No. 2015M581782), which are gratefully acknowledged.

References

Allotey, N. and El Naggar, M. H. (2008). "A numerical study into lateral cyclic nonlinear soil-pile response." *Canadian Geotechnical Journal*, Vol. 45, No. 9, pp. 1268-1281, DOI: 10.1139/T08-050.

Ashour, M., Norris, G., and Shamsabadi, A. (2001). "Effect of the nonlinear behavior of pile material on the response of laterally loaded piles." *Proceedings of 4th International Conference on Recent Advances in Geotechnical Earthquake Engineering and Soil Dynamics,* San Diego, Paper 6.10.

Basu, D., Salgado, R., and Prezzi, M. (2008). *Analysis of laterally loaded piles in multilayered soil deposits*, Joint Transportation Research Program.

Biocchi, N. (2011). *Structural and geotechnical interpretation of strain gauge data from laterally loaded reinforced concrete piles*. Doctoral dissertation, University of Southampton.

Chen, W. F. and Duan, L. (2003). *Bridge Engineering: Seismic Design*, CRC press.

Conte, E., Troncone, A., and Vena, M. (2013). "Nonlinear three-dimensional analysis of reinforced concrete piles subjected to horizontal loading." *Computers and Geotechnics*, Vol. 49, pp. 123-133, DOI: 10.1016/j.compgeo.2012.10.013.

El Naggar, M. H., Shayanfar, M. A., Kimiaei, M., and Aghakouchak, A. A. (2005). "Simplified BNWF model for nonlinear seismic response analysis of offshore piles with nonlinear input ground motion analysis." *Canadian Geotechnical Journal*, Vol. 42, No. 2, pp. 365-380, DOI: 10.1139/t04-103.

Fish, J. and Belytschko, T. (2007). *A first course in finite elements*, John Wiley & Sons.

Giannakos, S., Gerolymos, N., and Gazetas, G. (2012). "Cyclic lateral response of piles in dry sand: Finite element modeling and validation." *Computers and Geotechnics*, Vol. 44, pp. 116-131, DOI: 10.1016/j.compgeo.2012.03.013.

Heidari, M., Jahanandish, M., El Naggar, H., and Ghahramani, A. (2013). "Nonlinear cyclic behavior of laterally loaded pile in cohesive soil." *Canadian Geotechnical Journal*, Vol. 51, No. 2, pp. 129-143, DOI: 10.1139/cgj-2013-0099.

Heiniö, M. (1999). *Rock excavation handbook for civil engineering*, Sandvik Tamrock Corp.

Hsueh, C.-K., Lin, S.-S., and Chern, S.-G. (2004). "Lateral performance of drilled shaft considering nonlinear soil and structure material behavior." *Journal of Marine Science and Technology*, Vol. 12, No. 1, pp. 62-70.

Huang, A. B., Hsueh, C. K., O'neill, M.W., Chern, S., and Chen, C. (2001). "Effects of construction on laterally loaded pile groups." *Journal of Geotechnical and Geoenvironmental Engineering*, Vol. 127, No. 5, pp. 385-397, DOI: 10.1061/(ASCE)1090-0241(2001) 127:5(385).

Kim, Y., Jeong, S., and Lee, S. (2011). "Wedge failure analysis of soil resistance on laterally loaded piles in clay." *Journal of Geotechnical and Geoenvironmental Engineering*, Vol. 137, No. 7, pp. 678-694, DOI: 10.1061/(ASCE)GT.1943-5606.0000481, 678-694.

Liang, R. Y. (1997). *Pressuremeter to predict the lateral load capacity of drilled shafts on slopes,* A research report submitted to the Ohio Department of Transportation and FHWA.

Mander, J., Priestley, M., and Park, R. (1988). "Theoretical stress-strain model for confined concrete." *Journal of Structural Engineering*, Vol. 114, No. 8, pp. 1804-1826, DOI: 10.1061/(ASCE)0733-9445 (1988)114:8(1804).

Memarpour, M. M., Kimiaei, M., Shayanfar, M., and Khanzadi, M. (2012). "Cyclic lateral response of pile foundations in offshore platforms." *Computers and Geotechnics*, Vol. 42, pp. 180-192, DOI: 10.1016/j.compgeo.2011.12.007.

Nip, D. C. N. and Ng, C. W. W. (2005). "Back-analysis of laterally loaded bored piles." *Proceedings of the ICE-Geotechnical* Engineering, Vol. 158, No. 2, pp. 63-73, DOI: 10.1680/geng.2005.158.2.63.

O'neill, M. W. and Huang, A. B. (2003). "Comparative behavior of laterally loaded groups of bored and driven piles in cohesionless soil." *Proceedings of The 13th International Offshore and Polar Engineering Conference*, Hawaii,USA, pp. 25-30.

Paulay, T. and Priestley, M. J. N. (1992). *Seismic design of reinforced concrete and masonry buildings*, John Wiley & Sons, Inc.

Peng, J. R., Rouainia, M., and Clarke, B. G. (2010). "Finite element analysis of laterally loaded fin piles." *Computers & Structures*, Vol. 88, No. 21, pp. 1239-1247, DOI: 10.1016/j.compstruc.2010.07.002.

Poulos, H. G. (1971). "Behavior of laterally loaded piles I. single piles." *Journal of the Soil Mechanics and Foundations Division*, ASCE, Vol. 97, No. 5, pp. 711-731.

Prakash, S., and Kumar, S. (1996). "Nonlinear lateral pile deflection prediction in sands." *Journal of Geotechnical Engineering*, Vol. 22, No. 2, pp. 130-138, DOI: 10.1061/(ASCE)0733-9410(1996)122:2(130).

Priestley, M. J. N., Seible, F., and Calvi, G. M. (1996). *Seismic Design and Retrofit of Bridges*, John Wiley & Sons, New York.

Reese, L. C. (1984). *Handbook on design of piles and drilled shafts under lateral load*, Report No. FHWA-IP-84-11, University of Texas at Austin.

Reese, L. C. and Van Impe, W. F. (2001). *Single piles and pile groups under lateral loading*, Taylor & Francis Group plc, London, UK.

Reese, L. C. and Wang, S. T. (1994). "Analysis of piles under lateral loading with nonlinear flexural rigidity." *Proceedings of International Conference on Design and Construction of Deep Foundation*.

Reese, L. C. and Welch, R. C. (1975). "Lateral loading of deep foundations in stiff clay." *Journal of the Geotechnical Engineering Division*, Vol. 101, No. 7, pp. 633-649.

Reuss, R., Wang, S. T., and Reese, L. C. (1992). "Tests of piles under lateral loading at the pyramid building, memphis, tennessee." *Geotechnical News*, Vol. 10, No. 4, pp. 44-49.

Robert, Y. L., Ehab, S. S., and Jamal, N. (2007). "Hyperbolic *p-y* Criterion for Cohesive Soils." *Jordan Journal of Civil Engineering*, Vol. 1, No. 1, pp. 38-58.

Technical code for building pile foundation of China (JGJ 94 – 2008). Ministry of Housing and Urban-rural Development of the People's Republic of China, 2008.

Tuladhar, R., Maki, T., and Mutsuyoshi, H. (2008). "Cyclic behavior of laterally loaded concrete piles embedded into cohesive soil." *Earthquake Engineering & Structural Dynamics*, Vol. 37, No. 1, pp. 43-59, DOI: 10.1002/eqe.744.

Xu, L. Y., Cai, F., Wang, G. X., and Chen, G. X. (2016). "Nonlinear analysis of single laterally loaded piles in clays using modified strain wedge model." *International Journal of Civil Engineering*, DOI: 10.1007/s40999-016-0072-8.

Xu, L.Y., Cai, F., Wang, G. X., and Ugai, K. (2013). "Nonlinear analysis of laterally loaded single piles in sand using modified strain wedge model." *Computer and Geotechnics*, Vol. 51, pp. 60-71, DOI: 10.1016/j.compgeo.2013.01.003.

Zienkiewicz, O. Z., and Taylor, R. L. (2005). *The Finite Element Method for Solid and Structural Mechanics*, Sixth Edition, Elsevier Butterworth-Heinemann.